BROADBAND IMPEDANCE OF THE *NESTOR* STORAGE RING

V.P. Androsov, P.I. Gladkikh, A.M. Gvozd, I.M. Karnaukhov, Yu.N. Telegin*

National Science Center "Kharkov Institute of Physics and Technology", 61108, Kharkov, Ukraine

(Received April 12, 2011)

The contributions from lossy and inductive vacuum chamber components to the broadband impedance of the NESTOR storage ring are obtained by using both low-frequency analytical approaches and computer simulations. As was expected considering the small ring circumference (15.44 m), the main contributions both to the longitudinal impedance $Z_\parallel/n$ and the loss factor k_{loss} come from the RF-cavity. Cavity impedance was also estimated with CST Microwave Studio (CST Studio Suite^{TM} 2006) by simulating coaxial wire method commonly used for impedance measurements. Both estimates agree well. Finally, we performed the simulations of a number of inductive elements with CST Particle Studio 2010 by using wake field solver. We have also evaluated the bunch length in NESTOR taking the conservative estimate of 3 Ohm for the ring broadband impedance and have found that the bunch length $\sigma_z = 0.5\,cm$ could be obtained in steady state operation mode for the designed bunch current of 10 mA and RF-voltage of 250 kV.

PACS: 29.20.Dh, 29.27.Bd

1. INTRODUCTION

At the design stage of any storage ring it is customary to study the effects of beam interaction with a vacuum chamber (or a beam-pipe) because these effects determine, for the most part, the bunch parameters and limit the stored beam current. Since pioneer work by Sessler and Vaccaro [1] these effects are treated in the frequency domain in terms of coupling impedances: longitudinal impedance, $Z_\parallel(\omega)$ and transverse impedance $Z_\perp(\omega)$. Generally, the beam current is characterized with higher moments which describe the dynamics of charge distribution in the bunch, and one has to match to all moments m=1,2,3... the corresponding impedances $Z_\parallel^m(\omega)$ and $Z_\perp^m(\omega)$ (see, for example, [2]). In practice only impedances with m=0,1 which describe rigid bunch movement are studied in order to optimize the design of beam-pipe components and to consider the forthcoming beam instabilities and their possible cures. In this paper we consider the longitudinal broadband impedance which determines the bunch length in the NESTOR ring.

The longitudinal impedance is related to longitudinal beam component (m=0), which for a point charge is $I_z = I_0\delta(x-x_1)\delta(y-y_1)\exp(-i\frac{\omega}{c}z)$, and can be expressed in the following way:

$$Z_\parallel(\omega) \equiv Z_\parallel^0(\omega) = -\frac{1}{I_0}\int\limits_{-\infty}^{\infty} E_z e^{-j\omega c/z} dz\ , \qquad (1)$$

where E_z is the longitudinal component of the electric field along the beam axis, c is velocity of light.

For convenience, one usually consider broadband (BB) ring impedance, that corresponds to all low-Q components of the beam chamber, and narrow-band resonances originated from high-Q elements, first of all, RF-cavities. RF-cavities along with fundamental (accelerating) mode TM_{010} have a whole spectrum of higher order modes (HOM's) which can drive coupled-bunch instabilities (CBI) [3]. Cavity HOM's as a possible origin of CBI in the NESTOR were discussed in the previous paper [4].

Longitudinal broadband impedance is usually normalized to a harmonic number $n = \omega/\omega_0$, where ω_0 is a rotation frequency, and is expressed as $Z_\parallel/n$. For many beam-pipe elements $Z_\parallel(\omega)$ is inductive, so it is supposed that $Z_\parallel(\omega)/n$ is constant in a wide frequency range. $Z_\parallel/n$ is used for estimation of single-bunch instability thresholds with help of half-empirical criteria obtained in low-frequency approximation ($\omega \ll c/\sigma_z$, where σ_z is a bunch length). Obtained with this approach, Keil-Schnell-Boussard criterion [5] relates $Z_\parallel/n$ to the microwave instability threshold:

$$\left|\frac{Z_\parallel}{n}\right| < \frac{2\pi\alpha(\epsilon_0/e)\delta_\epsilon^2}{I_{peak}}\ , \qquad (2)$$

where α is the momentum compaction factor, ϵ_0 is the electron beam energy, e is electron charge and δ_ϵ is the relative beam energy spread. I_{peak} represents the bunch peak current which for the gaussian bunch of length σ_z is $I_{peak} = I_{av}\sqrt{2\pi r_0/\sigma_z}$, where I_{av} is the average bunch current and r_0 is the average radius of the ring. This approximation is good for a medium bunch length: $\sigma_z \le b$, where b is the

*Corresponding author. E-mail address: telegin@kipt.kharkov.ua

characteristic transverse size of the beam pipe. For short bunches ($\sigma_z \ll c/\omega_r$) one has to use in Eq.(2) instead of the low-frequency impedance $Z_\parallel/n$ the effective impedance $(Z_\parallel/n)_{eff}$, which is averaged over bunch frequency spectrum, thus taking into account that at high frequencies the bunch does not interacts with the low-frequency part of broadband impedance.

The real part of BB impedance determines beam energy losses. Parasitic energy loss per turn due to bunch-environment interaction is proportional to the bunch charge squared ($\Delta\epsilon = -k_{loss}q^2$), where factor k_{loss} is a loss parameter which for gaussian bunch can be presented as follows:

$$k_{loss} = \frac{1}{2\pi}\int\limits_{-\infty}^{\infty} ReZ_\parallel(\omega)\exp(-\frac{\omega^2\sigma_z^2}{c^2})dz\ . \qquad (3)$$

Below the cut-off frequency of a beam-pipe, ω_{cut}, broadband impedance is an additive value and the sum of contributions from various vacuum chamber components (so called "impedance budget") is usually evaluated in order to minimize this value.

Total parasitic energy losses have to be considered in designing of heat-removing circuits and in developing of the RF-system as a whole. The latter is especially important for low-energy rings like NESTOR, in which the parasitic losses exceed synchrotron radiation losses and define the synchronous phase of the beam.

We have evaluated contributions from various beam-pipe components to the longitudinal BB impedance of the NESTOR ring which is under construction in NSC KIPT [6]. Both analytical formulas and simulation codes were used for this purpose. The obtained data were used for evaluating the bunch lengthening in NESTOR due to microwave instability. The preliminary results were presented in the e-preprint [7].

In this paper we present the main results of this electronic paper together with new estimates of $Z_\parallel/n$ and k_{loss} obtained recently with new version of CST Studio [8].

2. THE BROADBAND IMPEDANCE OF THE *NESTOR* RING. ANALYTICAL APPROACH

The next ring components can give a substantial contribution to the ring broadband impedance:

– resistive wall;
– RF-cavity;
– pumping holes in dipole vacuum chambers;
– injection section with inflector chamber;
– beam pick-up's;
– holes in the laser-electron beam crossing chamber;
– RF-liners (bellows);
– flanges and welding joints.

2.1. THE RESISTIVE WALL IMPEDANCE

The resistive wall coupling impedance of a beam-pipe of elliptical cross section with major and minor semiaxes a and b can be evaluated with the following equation [9]:

$$\frac{Z_\parallel^{RW}}{n} = \frac{Z_0\delta}{2b}\frac{L}{2\pi r_0}(1+j)G_0(q)\ , \qquad (4)$$

where L is the pipe length, $\delta = (2c\rho/\omega Z_0)^{1/2}$ is the skin depth of the wall material whose specific resistance is ρ, Z_0 is the impedance of free space. $G_0(q)$ is a function of the parameter $q = (a-b)/(a+b)$ and is calculated via elliptic integrals and Jacobi elliptic functions. For NESTOR q=0.49, function $G_0(q) \approx 1$ and the resistive wall impedance is given by a simple equation: $Z_\parallel^{RW} = 1.35(1+i)\sqrt{n}\,[Ohm]$.

The resistive wall impedance $Z_\parallel^{RW}/n$ is traditionally evaluated at the roll-off frequency, $\omega_{roll-off}$ (the frequency at which the bunch spectrum power density $|\tilde{\rho}(\omega)|^2$ is one half of its peak value). For gaussian bunch $\omega_{roll-off} = c\sqrt{2}/\sigma_z$ and for the bunch length σ_z=1 cm ($\omega_{roll-off} \approx 25\,GHz$) the resistive wall impedance $Z_\parallel^{RW}/n$ amounts approximately to $0.13\,Ohm$.

The estimate for k_{loss}^{RW} according to Eq.(3) gives $0.06\,V/pC$ for bunch length $\sigma_z = 1\,cm$.

2.2. THE RF-CAVITY

The contribution from the RF-cavity HOM's (Higher Order Modes) to the ring broadband impedance can be estimated by using the following equation [10]:

$$\frac{Z_\parallel^{HOM}}{n} = \sum_i \left(\frac{R}{Q}\right)_i \cdot \frac{\omega_0}{\omega_i}\ , \qquad (5)$$

where ω_i and $(R/Q)_i$ are the resonance frequency and R/Q factor for the cavity mode with mode index i. The sum is taken over all HOM's with resonance frequencies lower than ω_{cut}. HOM's parameters were calculated with ANSYS code [11] using approach described elsewhere [4]. The estimation gives $Z_\parallel^{HOM}/n = 1.40\,Ohm$.

Cavity HOM's give a significant contribution to the total loss factor. This contribution was estimated as sum of energy losses over all cavity HOM's:

$$k_{loss}^{HOM} = \sum_i \left(\frac{R}{Q}\right)_i \cdot \omega_i \cdot \exp\left(-\frac{\omega^2\sigma_z^2}{c^2}\right)\ . \qquad (6)$$

It gives $k_{loss}^{HOM} = 0.48\,V/pC$ for bunch length $\sigma_z = 1\,cm$ and $0.54\,V/pC$ for $\sigma_z = 0.5\,cm$. Energy loss at fundamental mode doesn't depend on bunch length in this range of σ_z and amounts to $0.54\,V/pC$.

2.3. BEAM POSITION MONITORS

The beam position monitor (pick-up) represents four electrostatic electrodes - buttons - placed on the inside surface of the beam-pipe and separated from the latter by a narrow annular slot. The beam-pipe cross section at pick-up location is given in the Fig.1. Impedance of one button can be estimated as impedance

of an annular slot in the elliptic beam-pipe. The longitudinal impedance of of a hole in an elliptic beam-pipe in static approximation (hole dimensions are small compared with the wavelength) is given by [12]:

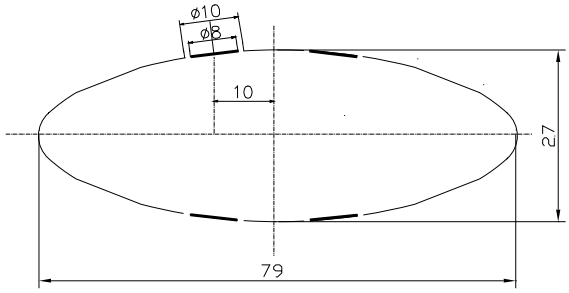

Fig.1. *Beam pipe cross section at pick-up location*

$$Z_{\parallel}^{hole} = \frac{j\omega Z_0}{8\pi^2 c} \cdot \frac{1}{a^2+b^2} \cdot \frac{(\psi_v - \chi)\cdot F_0^2(v)}{\sinh^2 u_0 + \sin^2 v} \qquad (7a)$$

$$F_0(v) = \frac{2K(k)}{\pi} \cdot \frac{k'}{dn(\overline{v},q)}\,, \qquad (7b)$$

where ψ_v and χ are the susceptibility and polarizability of the hole; v is an azimuthal elliptic coordinate; u_0 is related to ellipse semi-axes via: $\cosh u_0 = a/\sqrt{a^2-b^2}$; $dn(\overline{v},q)$ is Jacobi elliptic function of the argument $\overline{v} = 2K(k)v/\pi$); $K(k)$ is the complete elliptic integral of the first kind; $k' = \sqrt{1-k^2}$ and q is defined above. The azimuthal elliptic coordinate of the button center is $v = 75.3^0$ and $F_0(v)$=2.58.

The susceptibility ψ and polarizability χ of a narrow annular slot ($w = r_{ext} - r_{int} \ll r_{ext}$, where r_{ext} and r_{int} are external and internal radii of the slot) in a thin wall are given by [13]:

$$\psi = \frac{\pi^2 r_{ext}^2 r_{int}}{\ln(32 r_{ext}/w) - 2}\,, \qquad (8a)$$

$$\chi = -\frac{1}{8}\pi^2 w^2 (r_{ext} + r_{int})\,. \qquad (8b)$$

Calculations give $Z_{\parallel}^{BPM}/n = 1.1\cdot 10^{-2}\,Ohm$ for one pick-up (4 buttons). It should be noted that the value of pick-up impedance obtained as a difference of impedances of two circular holes with radii r_{ext} and r_{int} [14] is four times less than the value given above.

For estimation of the real part of the pick-up impedance we used the formula obtained for a circular beam-pipe [15] and modified in accordance with Eq.(7):

$$Re Z_{\parallel}^{hole} = Z_0 \Big(\frac{\omega}{c}\Big)^4 \frac{(\psi_v^2 + \chi^2)\cdot F_0^2(v)}{96\pi^3\left[b^2 + (a^2-b^2)\sin^2 v\right]}\,, \qquad (9)$$

where $F_0(v)$ is defined by Eq.(7). The loss parameter is given by:

$$k_{loss}^{hole} = \frac{Z_0\sqrt{\pi}}{16\pi^4\sigma_z^5} \cdot \frac{(\psi_v^2 + \chi^2)\cdot F_0^2(v)}{b^2 + (a^2-b^2)\sin^2 v}\,. \qquad (10)$$

Calculation gives $k_{loss}^{BPM} = 6.8\cdot 10^{-5}\sigma_z[cm]^{-5}\,V/pC$ for one pick-up.

3. THE BROADBAND IMPEDANCE OF THE *NESTOR* RING. COMPUTER SIMULATIONS

3.1 SIMULATIONS WITH CST MICROWAVE STUDIO

For some beam pipe elements the BB impedance couldn't be estimated analytically. Such are pumping slots in the vacuum chamber of dipole magnet, which have transverse dimensions comparable to those of the beam pipe. At the beginning of our studies we have tried to estimate their impedance by simulating coaxial wire method, widely used for impedance bench measurements [16], with CST MWS code (CST Studio Suite^{TM} 2006).

The basic concept of this method relies on substituting the beam by a thin wire and thus simulating the fields of ultrarelativistic beam on the beam pipe wall by the propagation of TEM mode in the transmission line so formed. In the transmission line framework a single, lumped wall impedance Z_W can be expressed in terms of S-matrix coefficients in the following way:

$$S_{11} = \frac{Z_W}{2Z_c + Z_W} \quad \text{and} \quad S_{21} = \frac{2Z_c}{2Z_c + Z_W}\,, \qquad (11)$$

where Z_c is characteristic impedance of the transmission line. In principle either coefficient can be used for impedance determination, but the transmission coefficient is applicable in more general configurations and is usually preferred in bench measurements.

The question to what degree the simulated impedance Z_W approximate the BB impedance is raised from time to time [17, 18]. A good agreement between calculations and measurements has been shown for a simple cavity-like structure with a thin wire ($d = 0.75\,mm$) [17].

As the first step we applied this approach to estimate the broadband impedance of the RF-cavity and to compare it to that obtained with analytical approach.

The simplified cavity model (without ports) used in simulations is shown in Fig.2. The calculated S-parameters in the frequency range 1...5 GHz are presented in Fig.3.

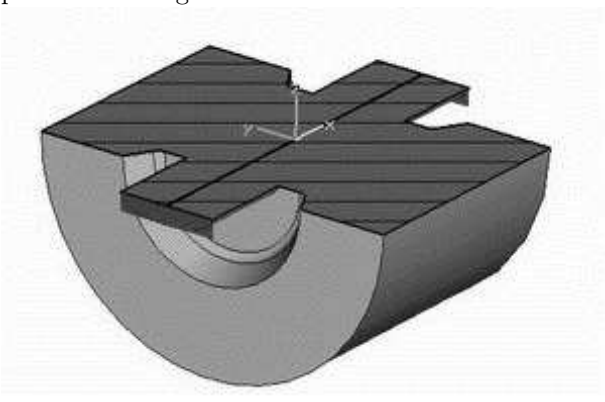

Fig.2. *Cavity model used in simulations*

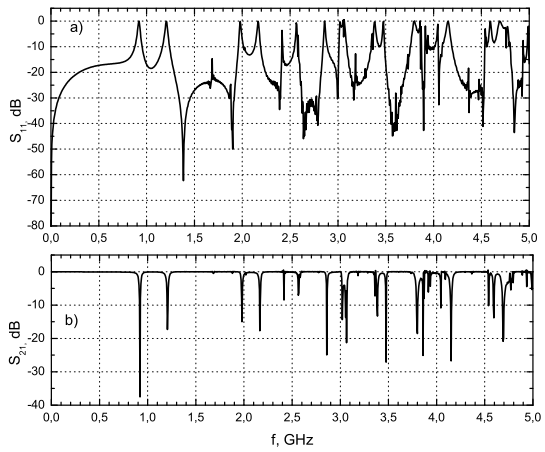

Fig.3. *Scattering matrix parameters: a) S_{11} (reflection) and b) S_{21} (transmission)*

The analysis of the electromagnetic field distribution at resonance frequencies (minima in S_{21}) reveals:

1. The field patterns at resonance frequencies in peripheral region are similar to that of cavity modes. In particular, first resonance corresponds to TM_{010} mode but the mode frequency is shifted to higher frequencies. The field in the output beam pipe is zero i.e. the cavity acts as a notch filter.

2. At frequencies corresponding to minima in S_{11} the electromagnetic wave doesn't excite the cavity (field in peripheral region is zero) and the structure behaves as an usual coaxial transmission line.

Cavity impedance obtained from S_{21} with Eq.(11) is presented in Fig.4. To show small peaks in the spectrum the latter is stretched along Y-axis so two large peaks are cut off. Contribution to the ring broadband impedance from cavity HOM's was calculated with the following expression:

$$Z_{\parallel}^{HOM}/n = \frac{1}{f_{cut} - f_c} \cdot \int_{f_c}^{f_{cut}} Z_W(f) \frac{f_0}{f} df \qquad (12)$$

Bottom limit of integration f_c was taken in the minimum between the first and the second resonances. The integration was performed up to $f_{cut} = 5.9\,GHz$ (this value was also obtained with CST MWS).

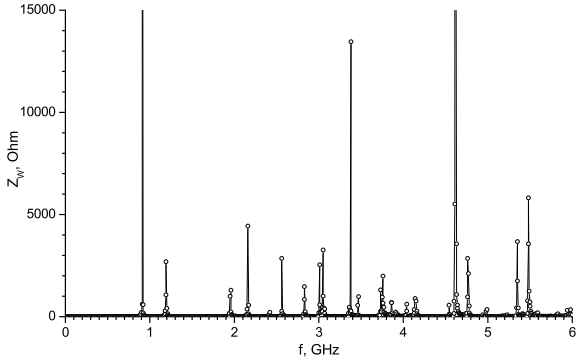

Fig.4. *Cavity impedance*

The obtained value $Z_{\parallel}^{HOM}/n = 1.29\,Ohm$ well agrees with the estimate obtained with analytical approach (see 2.2).

Our efforts to obtain the contribution to BB-impedance from pumping holes in dipole chamber by using this approach were not so successful, we could only estimate the upper limit: $Z_{\parallel}/n < 0.05\,Ohm$ for one chamber (see ref. [7]).

3.2 SIMULATIONS WITH CST PARTICLE STUDIO (CST STUDIO SUITE^{TM} 2010)

At the final stage of our studies the impedances of a number of inductive elements (the pumping holes in the vacuum chamber of dipole magnet, RF-liner, strip-line pickup, the slot between welding membranes) were obtained with CST Particle Studio 2010 by using the wake field solver and FFT (Fast Fourier Transform). The BB impedance $Z_{\parallel}/n$ was obtained from calculated $Z(f)$ with the Eq.(12)(taking $f_c = 0$), the loss factor values were directly calculated by the code. All simulations were performed for a $10\,mm$ bunch and wake lengths $s = 10\,cm$ and $s = 50\,cm$

3.2.1. THE CHAMBER OF THE DIPOLE MAGNET

The cross section of the main chamber in the dipole magnet is similar to that in a straight section. The main chamber is joined to the antechamber through 16 elliptical holes with axes dimensions of $22\,mm$ and $14\,mm$. Two chambers from a whole number of four differ in their design by presence of additional holes for electron beam injection or X-ray beam extraction. Fig.5 shows a segment of the dipole vacuum chamber with two holes.

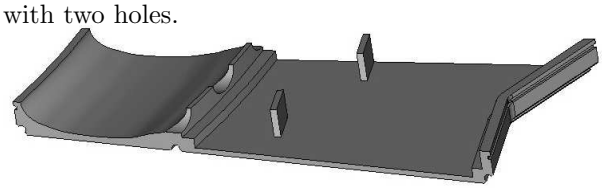

Fig.5. *The segment of vacuum chamber in the dipole magnet (bottom half)*

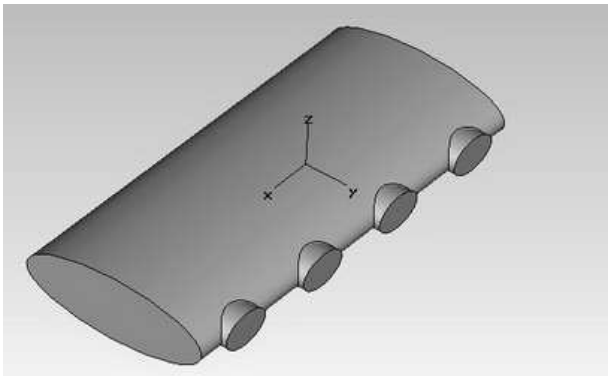

Fig.6. *The model of dipole chamber segment with 4 holes used in simulations*

Fig.6. shows the model used in simulations which represents the internal volume of the "straightened"

segment of the main chamber with holes between main chamber and antechamber. In simulations this volume (vacuum) is surrounded with PEC background material except holes, where open boundary conditions are imposed (electromagnetic energy can radiate through holes).

In order to exclude the possibility of the effects of interference between holes we simulated the chamber segments with a different number of holes (n=1,2,3,4). Fig.7 shows the calculated wake function for the 4-hole segment and the normalized distribution of the bunch charge for reference. Fig.8 presents the real and imaginary parts of calculated impedance $Z(f)$ for that segment. One can see that the real part is negligibly small in this frequency range.

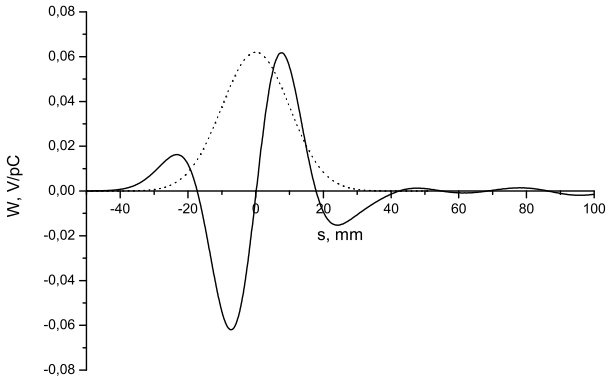

Fig.7. *Wake function (solid line) and bunch charge distribution (dotted line) for the 4-hole segment*

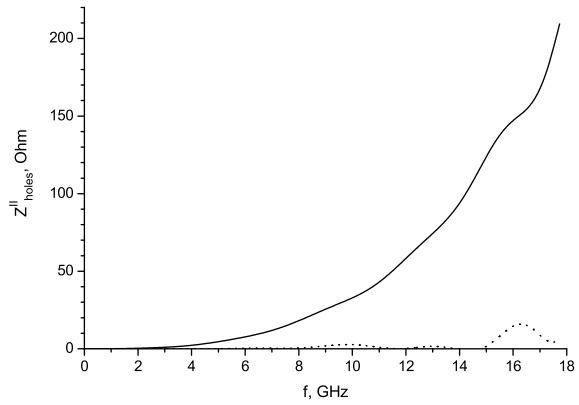

Fig.8. *The real (solid line) and imaginary (dotted line) parts of $Z^{\parallel}_{holes}(f)$ for the 4-hole segment*

Fig.9 shows the dependence of $Z_{\parallel}/n$ versus number of holes. The linear fit to obtained data does not show interference between holes (at least up to f_{cut}), so the BB impedance of the dipole chamber can be obtained as the sum of impedances of single-hole segments.

The simulations give $Z_{\parallel}/n = 0.033\,Ohm$ and $k_{loss} = 0.002\,V/pC$ for the single chamber. It should be noted that the value of $Z_{\parallel}/n$ well agrees with the estimate for the upper limit given in 3.1.

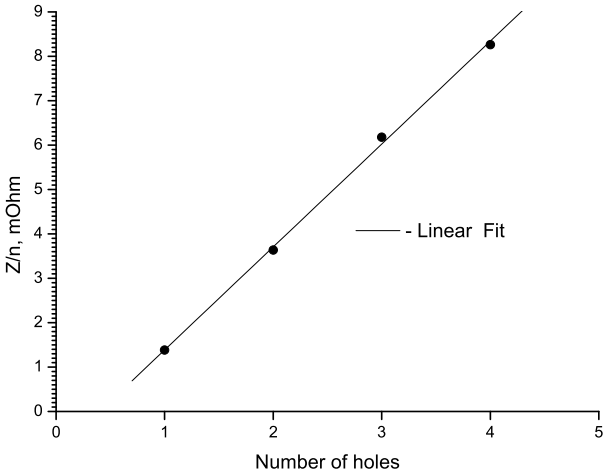

Fig.9. *Impedance of the dipole chamber segment versus number of holes. The line is linear fit to obtained data (points)*

3.2 2. THE STRIP-LINE PICKUP

The strip-line pickup represents four wires ($d = 3\,mm$, $l = 105\,mm$) stretched in the longitudinal groves ($d = 7\,mm$) milled out in the chamber wall. The model of strip line pickup, used in simulations, with the cross section taken through two wires is given in Fig.10.

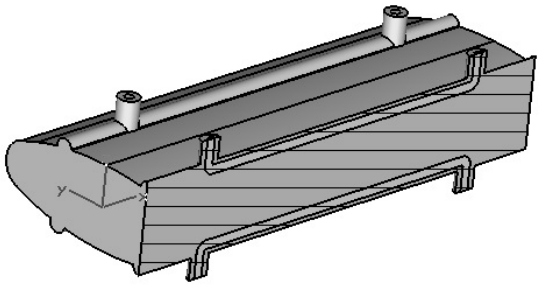

Fig.10. *The strip-line pickup model used in the simulation*

The simulations give $Z_{\parallel}/n = 0.012\,Ohm$ and $k_{loss} = 0.003\,V/pC$.

3.2.3. THE VACUUM CHAMBER JOINTS AND RF-SHIELDS

The various elements of the NESTOR vacuum chamber are joined together by two ways: by flange joints and by welding. In the former case the vacuum joint incorporates bellows with circular cross section, so the RF-shield is used to reduce coupling impedance of the bellows. This shield represents a piece of elliptic tube with 22 pumping slots $3\,mm$ wide and $80\,mm$ long, equidistantly distributed along tube circumference. On the one side the shield is welded to the bellows flange and on the other side it tightly fits into the adjacent piece of the beam pipe thus bridging the bellows gap and providing the required RF-contact.

In the latter case the adjacent sections of the stainless-still beam-pipe are joined together by welding for which operation there are membranes at section ends. After welding between two joined sections

an annular gap $\sim 1.0\,mm$ wide and $4\,mm$ deep is formed.

Simulation models for both type of vacuum joints are given in Fig.11.

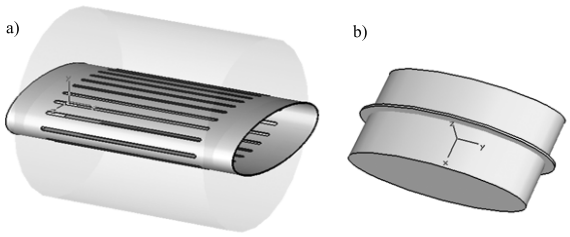

Fig.11. *Simulation models for the bellows RF-shield (a) and welding joint (b)*

The simulation results are presented in the next section.

4.THE BROADBAND IMPEDANCE OF THE *NESTOR* RING. RESULTS

The obtained results are summarized in Tables 1,2. As follows from the tables for bunch length considered ($\sigma_z = 0.5, 1.0\,cm$) the main contribution both to longitudinal broadband impedance and loss factor comes from the RF-cavity. From a comparison of the loss factor data for two bunch lengthes one can see how the contributions from other components are increased with bunch shortening while the contribution from the RF-cavity isn't changed essentially.

Table 1. *Longitudinal broadband impedance budget*

Component	N	$\lvert Z_\parallel/n\rvert, Ohm$		
		Anal.	CST MWS 2006	CST PS 2010
RF-cavity	1	1.40	1.29	
Res. wall	1	0.13		
Dipole	4		< 0.20	0.13
BPM	2	0.02		
Weld. joint	8	0.04		0.21
RF-shield	4	0.003		0.11
Strip line	1			0.01
Total		2.01		

Table 2. *Loss factors of beam pipe components*

Component	N	$k_{loss}, V/pC$		
		$\sigma_z = 1\,cm$		$\sigma_z = 0.5\,cm$
		Anal.	CST	Anal.
RF-cavity	1	1.02	1.04	1.08
Res. wall	1	0.06		0.17
Dipole	4		0.008	
BPM	2	0.0002		0.0044
Weld. joint	8		0.08	
RF-shield	4		0.008	
Strip line	1		0.003	
Total		1.2		> 1.3

It should be mentioned that for the time being we have no estimates for the following components: i) the beam-pipe section for the crossing point of the electron and laser beams; ii) the injection section (inflector); iii) the DC monitor assembly, that includes a circular ceramic ring and bellows with RF-shields. The first element at the commissioning stage will be replaced with a straight section. The injection section is essentially non-symmetric, it gives, presumably, a substantial contribution to broadband impedance and so it requires to be studied with 3D time-domain codes.

5. TURBULENT BUNCH LENGTHENING IN THE *NESTOR* STORAGE RING

There are two mechanisms of bunch lengthening in cyclic accelerators. The first one is caused by the potential well distortion [2] and can lead to both bunch lengthening (inductive impedance) and bunch shortening (capacitive impedance). The estimates show that for NESTOR this effect is negligible.

The second one is usually explained by coherent mode coupling effect arising through overlapping of mode frequencies at high bunch currents. This effect displays itself as a longitudinal instability (microwave instability [19]), leads to turbulent bunch lengthening, observed at bunch currents higher than some threshold value, and is accompanied with growth of the beam energy spread.

The threshold bunch current I_{av}^{th} for a given value of $Z_\parallel/n$ can be obtained with Eq.(2). Above threshold the bunch length can be estimated with the equation [20]:

$$\sigma_z^{tbl} = r_0 \left(\sqrt{2\pi} \left| \frac{Z_\parallel}{n} \right| \frac{I_{av}}{h V_c \sin \Phi_s} \right)^{1/3}, \qquad (13)$$

where h is the harmonic number, V_c is the amplitude of RF-voltage and Φ_s is the synchronous phase of the beam. One can see from Eq.(13) that the bunch length doesn't depend on the electron beam energy above the instability threshold.

It should be noted that all these equations are obtained in the low-frequency approximation and they are valid for the inductive impedance and medium bunch lengths ($\sigma_z \geq$ 1cm). We estimated bunch lengths for a reasonable range of RF-voltages. NESTOR parameters used in these calculations are presented in Table 3, the obtained results are given in Table 4.

Table 3. *NESTOR ring parameters*

Parameter	Units	value
Average radius, r_0	m	2.46
Harmonic number, h		36
Compaction factor, α		0.01
Bunch current (maximal), I_{av}	mA	10
Ring broadband impedance, $Z_\parallel/n$	Ohm	3.0
Synchronous phase, Φ_s	deg	89

Table 4. *Bunch length in NESTOR*

V_c, kV	$\epsilon_0 = 60\,MeV$			$\epsilon_0 = 250\,MeV$			σ_z^{tbl}, cm
	δ_E^{ibs}	σ_z^{ibs}, cm	I_{av}^{th}, mA	δ_E^{ibs}	σ_z^{ibs}, cm	I_{av}^{th}, mA	
10	$0.17 \cdot 10^{-2}$	1.32	7.7	$0.47 \cdot 10^{-3}$	0.71	1.2	1.46
50	$0.19 \cdot 10^{-2}$	0.67	5.1	$0.53 \cdot 10^{-3}$	0.36	0.8	0.85
180	$0.21 \cdot 10^{-2}$	0.40	3.7	$0.59 \cdot 10^{-3}$	0.21	0.6	0.56
250	$0.22 \cdot 10^{-2}$	0.34	3.4	$0.60 \cdot 10^{-3}$	0.18	0.5	0.50

In our calculations we have taken $Z_\parallel/n = 3\,Ohm$, that is factor 1.5 greater than the value given in the table, in order to make compensation for the contributions from beam-pipe components not considered in the paper, first of all, the inflector. The values of the energy spread δ_E^{ibs} and bunch length σ_z^{ibs} presented in Table 4 were calculated with DECA code [21], which takes into account the effect of intrabeam scattering (IBS) – electron-electron scattering in a bunch. The threshold currents obtained with Eq.(2) for these IBS-corrected bunch parameters are below the goal value of $10\,mA$ per bunch, so the bunch will be lengthening in the ring. For the designed RF-voltage of $250\,kV$ estimation gives $\sigma_z^{tbl} = 0.5\,cm$.

At the commissioning stage of the NESTOR project an RF-amplifier with output power of $1\,kW$ is available thus providing the accelerating voltage of $50\,kV$ and the stored beam currents of up to $100\,mA$. We have no equipment to control the filling pattern, so all 36 RF-buckets will be filled up, and the maximal bunch current will be decreased down to $3\,mA$. For this case estimation gives $\sigma_z^{tbl} = 0.6\,cm$.

6. CONCLUSIONS

The conservative estimate of the longitudinal broadband impedance of the NESTOR ring ($Z_\parallel/n = 3\,Ohm$) confirms the possibility of obtaining the bunch length of $0.5\,cm$ with the goal bunch current of $10\,mA$ for the designed RF-voltage of $250\,kW$. At the commissioning stage we can obtain $3\,m$A in a $0.6\,cm$ bunch with the RF-voltage of $50\,kV$.

References

1. A. Sessler, and V. Vaccaro. *Longitudinal instabilities of azimuthally uniform beams in circular vacuum chambers with walls of arbitrary electrical properties*: Preprint, CERN-ISR-67-02, 1967, 24 p.
2. A.W. Chao. *Physics of Collective Beam Instabilities in high energy accelerators.* New York: "John Wiley and Sons, Inc.", 1993, 371 p.
3. J.L. Laclare. Bunched beam coherent instabilities// *Proc. CERN Accel. School–1985.* Oxford, England, 1987, p. 264-236.
4. V.P. Androsov, et al. RF-cavity for the X-ray generator NESTOR// *PAST. Series: Nuclear Physics Investigations.* 2007, 5(48), p. 151-155.
5. D. Boussard. *Observation of microwave longitudinal instabilities in the CPS:* Preprint, CERN-LabII/RF/Int./75-2, 1975.
6. V.Androsov, et al. X ray generator based on Compton scattering // *Nucl.Instrum. and Meth.A.* 2005, v.543, p.58-84.
7. V.Androsov, et al. *Broadband impedance of the NESTOR storage ring* : e-preprint. http://arxiv.org/list/ arXiv:1006.4846v1 [physics.acc-ph] 24 Jun 2010.
8. CST Studio Suite^{TM} 2010. http://www.cst.com.
9. R.L. Gluckstern, and J. van Zeijts. Coupling impedance of beam pipes of general cross section // *Phys.Rev.E.* 1993, v.47, p.656-663.
10. Y.C. Chae, et al. Longitudinal coupling impedance of the APS storage ring // *Particle Accelerator Conference.* Portland, USA, 2003, p.3014-3016.
11. ANSYS. http://www.ansys.com.
12. R.L. Gluckstern, J. van Zeijts, and B. Zotter. *Coupling impedance of a hole in an elliptical beam pipe*: Preprint, CERN SL/AP 92-18, 1992, 12 p.
13. S.S. Kurennoy. *Polarizabilities of an annular cut and coupling impedances of button-type beam position monitors*: e-preprint, http://arXiv:acc-phys/9504003v1, 1995, 3 p.
14. S. Heifets, et al. Impedance study for the PEP-II B-factory // *KEK Proceedings 96-6, CEIBA95.* Tsukuba, Japan, 1996, p.23-93.
15. S.S. Kurennoy, and Yong Ho Chin. *Coupling impedances and heating due to slots in KEK B-factory*: e-preprint, http://arXiv:acc-phys/9502002, 1995, 14 p.
16. F. Caspers. *Handbook of Accelerator Physics and Engineering.* Singapore: "World Scientific", 1998, p.570.
17. V.G. Vaccaro, et al. Coaxial wire technique: a comparison between theory and experiment // *Nuovo Cimento.* 1999, v. B114. p.1319-1334.
18. H. Hahn. Interpretation of coupling impedance bench measurements. *Phys. Rev. ST, Accelerators and Beams.* 2004, v.7, p.012001.
19. F.J. Sacherer. Bunch lengthening and microwave instability // *IEEE Trans. Nucl. Sci.* 1977, N.S24, p. 1393-1395.

20. A.Hoffman. *Diagnostics and cures for beam instabilities*: Preprint, CERN-ISR-TH/80-35, 1980, 15 p.

21. A. Zelinsky, and P. Gladkich. New abilities of computer code DECA // *European Particle Accelerator Conference*. Luzern, Switzerland, 2004, p.2164-2166.

ШИРОКОПОЛОСНЫЙ ИМПЕДАНС НАКОПИТЕЛЯ *НЕСТОР*

В.П. Андросов, П.И. Гладких, А.М. Гвоздь, И.М. Карнаухов, Ю.Н. Телегин

Получены оценки вкладов в реальную и мнимую части широкополосного импеданса от различных компонент вакуумной камеры накопителя НЕСТОР с помощью как аналитических выражений, полученных в низкочастотном приближении, так и компьютерного моделирования. Как и ожидалось, исходя из того, что длина окружности кольца невелика ($15,44\,м$), основной вклад, как в продольный импеданс $Z_{\|}/n$, так и в фактор энергетических потерь k_{loss}, дает ВЧ-резонатор. Широкополосный импеданс резонатора был также получен с помощью CST Microwave Studio (CST Studio Suite^{TM} 2006) путем моделирования метода "коаксиальной проволоки" , широко используемого для измерения импеданса. Обе оценки хорошо согласуются между собой. Проведено моделирование ряда индуктивных элементов с помощью CST Particle Studio 2010, используя программу, вычисляющую кильватерные поля. Мы также оценили длину сгустка в накопителе, взяв консервативную оценку $Z_{\|}/n = 3\,Ом$, и показали, что для проектных величин тока в сгустке $10\,мА$ и амплитуды ВЧ-напряжения в резонаторе $250\,кВ$ длина сгустка составляет $\sigma_z = 0.5\,см$.

ШИРОКОСМУГОВИЙ ІМПЕДАНС НАКОПИЧУВАЧА *НЕСТОР*

В.П. Андросов, П.І. Гладких, А.М. Гвоздь, І.М. Карнаухов, Ю.М. Телегін

Одержані оцінки внесків в реальну та мниму частини широкосмугового імпедансу від різних компонент вакуумної камери накопичувача НЕСТОР за допомогою як аналітичних виразів, одержаних у низькочастотному наближенні, так і комп'ютерного моделювання. Як і очікувалось, виходячи з того, що довжина окружності кільця невелика ($15,44\,м$), основний внесок, як в поздовжний імпеданс $Z_{\|}/n$, так і в фактор енергетичних втрат k_{loss}, дає ВЧ-резонатор. Широкосмуговий імпеданс резонатора був також одержаний за допомогою CST Microwave Studio (CST Studio Suite^{TM} 2006) шляхом моделювання методу "коаксіального дроту" , який широко використовується для виміру імпеданса. Обидві оцінки добре узгоджуються між собою. Виконано моделювання декількох індуктивних елементів за допомогою CST Particle Studio 2010, використовуючи програму, що обчислює кільватерні поля. Мы також оцінили довжину згустка в накопичувачі, узявши консервативну оцінку $Z_{\|}/n = 3\,Ом$, та показали, що для проектних величин струму в згустку $10\,мА$ та амплітуди ВЧ-напруги в резонаторі $250\,кВ$ довжина згустку становить $\sigma_z = 0.5\,см$.